Indoor air quality evaluation in naturally cross-ventilated buildings for education using age of air

S F Díaz-Calderón[1], J A Castillo[2] and G Huelsz[1]

[1] Instituto de Energías Renovables, Universidad Nacional Autónoma de México
Priv. Xochicalco s/n, Col. Centro, 62580, Temixco, Mor., México
[2] Departamento de Arquitectura y Diseño, Universidad de Sonora, Blvd. Encinas y Rosales, Col. Centro, 83000, Hermosillo, Son., México

E-mail: sfdc@ier.unam.mx

Abstract. Natural ventilation (NV) is a strategy of bioclimatic design to promote hygrothermal comfort and indoor air quality (IAQ). Nowadays, COVID-19 pandemic highlights the review of ventilation standards. In Mexico, the IAQ standard states a minimum of 6 ACH for educational buildings. ACH considers NV as an ideal piston flow and does not provide information of indoor airflow distribution. In this work, new age of air associated parameters are proposed, considering the indoor airflow distribution: the air renovation per hour (ARH) and the renovation parameter R. An isolated educational building located in a rural region is studied. Four window configurations of cross-ventilation are considered. All configurations have one windward window located at bottom. The configurations axial and upward have one leeward window at bottom and top, respectively. While, configurations corner and upward corner have one lateral side window at bottom and top, respectively. A CFD model of the educational building is validated with experiments. The axial configuration has the best performance according to ACH, nevertheless has the worst performance according to ARH and R. The results show that NV evaluation using ACH can lead to wrong decisions. An improvement of NV standard with the age of air associated parameters is recommended.

1. Introduction

Natural ventilation (NV) is a strategy of bioclimatic design, mainly in warm conditions, to promote hygrothermal comfort and indoor air quality (IAQ) [1]. Along many years, this strategy has been widely applied to remove indoor pollutants and infectious particles. Nowadays, the COVID-19 pandemic is a new challenge for the indoor activities in the new normality [2]. NV in a building must be designed to achieve the safety values of IAQ. The parameter used for NV evaluation in terms of IAQ and its value depend on local standards of every country. In Mexico for educational buildings, the minimum value of air changes per hour (ACH [1/h]) is of 6 times per hour [3]. The ACH considers the natural ventilation as an ideal piston flow. NV is a complex phenomenon which can be analyzed considering the indoor airflow distribution as zones with air movement and air stagnation. The age of air associated parameters (AoA) are used to qualitatively identify air movement and air stagnation [4, 5]. In this work, the AoA are also used to quantitatively evaluate the indoor airflow distribution [6].

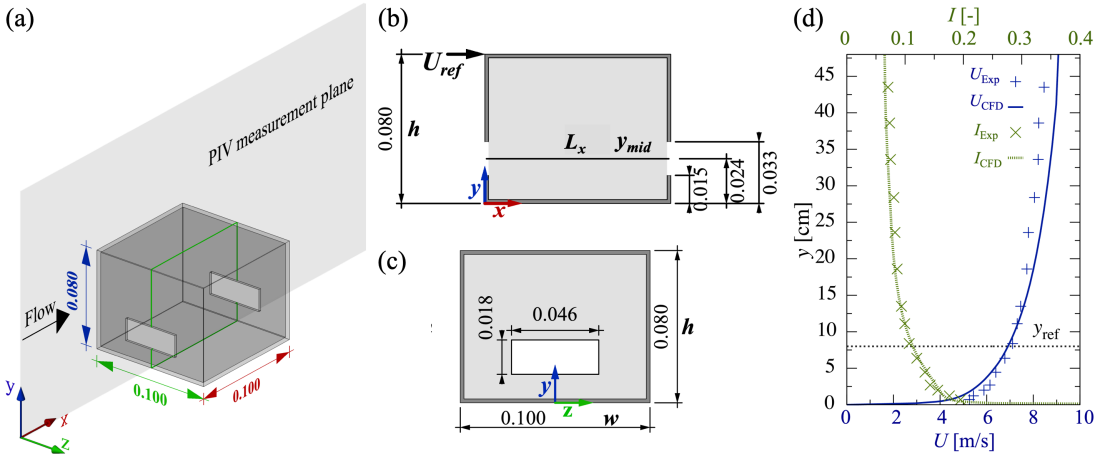

Figure 1. Cross-ventilation configuration of axial windows at bottom and $P = 0.10$ (reference case) with dimensions in m: (a) isometric with measurement vertical central plane, (b) lateral view and (c) front view; and (d) comparison of the velocity $U(y)$ and turbulence intensity $I(y)$ incident profiles from the experiment and from the CFD simulation.

This work presents the NV evaluation considering the indoor airflow distribution of an isolated educational building in a rural region of Mexico. Four cross-ventilation configurations of the most used location windows are tested. The study is performed using validated CFD simulations. A comparison of the ACH and AoA results is presented in order to remark the need of an improvement in the Mexican standards for NV.

2. Wind tunnel experiment

The wind tunnel experiments reported in [7] are used in the CFD validation. A laboratory scaled building with closable windows is used to reproduce different configurations of cross-ventilation. There are three window heights (bottom, middle and top) and three facade porosities P (0.05, 0.10 and 0.20, ratio between window and facade areas). The windows are located in oposite or lateral side facades. For all experiments, perpendicular wind direction to the windward facade is used. The Particle Image Velocimetry (PIV) technique is implemented to obtain two components of the velocity at the vertical central plane of the building. Figure 1a shows a scheme of the cross-ventilation configuration of axial windows at bottom and $P = 0.10$ (reference case) with the PIV measurement plane. The dimensions of the building are included (figure 1b, c). The Reynolds building number Re_b [-] is defined by

$$Re_b = \frac{U_{ref} y_{ref}}{\nu} = 3.56 \times 10^4, \tag{1}$$

where $U_{ref} = 6.97$ m/s is the reference velocity measured at the reference height $y_{ref} = 0.08$ m, and $\nu = 1.57 \times 10^{-5}$ m^2/s is the air viscosity. The velocity incident profile $U(y)$ is obtained by fitting the experimental measurements with the expression

$$U(y) = U_{ref} \left(\frac{y}{y_{ref}} \right)^{\alpha}, \tag{2}$$

where $\alpha = 0.12$ [-] is the exponential friction coefficient. Figure 1d shows $U(y)$ and the turbulence intensity $I(y)$ incident profiles without the building presence.

3. Evaluation parameters

In this work, contour plots of the normalized magnitude velocity U/U_{ref} [-] and velocity fields are obtained at vertical and horizontal planes to show the zones with air movement and air stagnation. The ACH (ideal piston flow consideration) is one of the most used NV evaluation parameters. The ACH does not consider the indoor airflow distribution and it is defined as

$$ACH = \frac{3600}{\tau_n}, \tag{3}$$

where $\tau_n = V/Q$ [s] is the nominal time, V [m^3] the indoor air volume and Q [m^3/s] the volumetric flow at outlet.

The AoA are an alternative to evaluate the NV considering the indoor airflow distribution [6]. The local mean age of air $\overline{\tau_i}$ [s] is the estimation of the time that a parcel of air at the building indoor has elapsed in the indoor since its entrance. To solve $\overline{\tau_i}$, a transport equation is defined in [6]

$$\left(\overline{u}\frac{\partial\overline{\tau_i}}{\partial x} + \overline{v}\frac{\partial\overline{\tau_i}}{\partial y} + \overline{w}\frac{\partial\overline{\tau_i}}{\partial z}\right) - \frac{\partial}{\partial x}\left(D_{ex}\frac{\partial\overline{\tau_i}}{\partial x}\right) - \frac{\partial}{\partial y}\left(D_{ey}\frac{\partial\overline{\tau_i}}{\partial y}\right) - \frac{\partial}{\partial z}\left(D_{ez}\frac{\partial\overline{\tau_i}}{\partial z}\right) = 1, \tag{4}$$

where $\overline{u}$, $\overline{v}$ and $\overline{w}$ are the velocity components known from the Navier-Stokes equations solution. The effective coefficients $D_{ej} = D_j + D_m$ (j = x, y and z) is the sum of the turbulent diffusivity D_j and the mass diffusivity D_m coefficients. The air renovation time $\langle\tau_r\rangle = 2\langle\tau_i\rangle$ [s], where $\langle\tau_i\rangle$ [s] is the spatial average of $\overline{\tau_i}$ in V.

In this work, two AoA are proposed: the air renovations per hour ARH [1/h] and the renovation parameter R [%]. ARH is calculated as

$$ARH = \frac{3600}{\langle\tau_r\rangle}. \tag{5}$$

R measures the percentage of the indoor air volume with $\overline{\tau_i}$ less than or equal to τ_n, *e.i.* the indoor air volume percentage with significant air movement,

$$R = \frac{V_{\overline{\tau_i}\leq\tau_n}}{V_{lz}}. \tag{6}$$

The indoor air volume with $\overline{\tau_i}$ above τ_n is considered to be without enough air movement related to air stagnation zones [6].

4. Considerations to obtain $\overline{\tau_i}$ in ANSYS Fluent 19.0

To solve equation 4, the flow solution must be previously calculated. The effective coefficients $D_{ej} = D_j + D_m$ are assigned employing a user define function. In [4], it is suggested to use $D_{ej} = \frac{\nu_t}{Sc_t} + (2.88 \times 10^{-5})\rho$, where ν_t is the turbulent viscosity, $Sc_t = \frac{\nu_t}{D_j}$ the turbulent Schmidt number and ρ [kg/m^3] the air density. For ventilation in low rise buildings, $Sc_t = 0.7$ is recommended [6]. For this work, a journal script is created to automatically and systematically obtain $\overline{\tau_i}$ [8].

5. CFD validation

The CFD simulations presented in this work are validated using the experimental data of [7]. The CFD validation is based on the methodology of the Best Practice Guidelines of Natural Ventilation CFD Simulations [9, 10, 11].

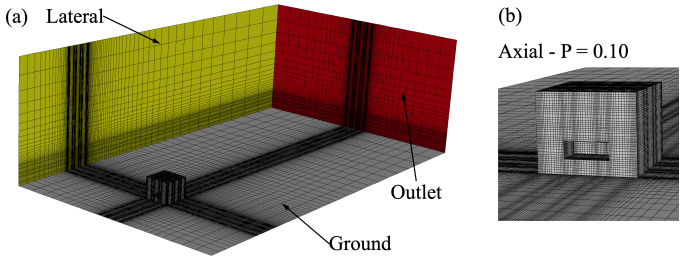

Figure 2. Perspective views of the computational domain, (a) with indications of the boundary type and (b) a close up of the building.

5.1. Computational domain

The computational domain is generated with the surface cell extrusion technique, resulting in a block-structured grid with hexahedral cells [12]. According to [13], the height of the first cell extrusion is $y_1 = 2.1\ k_s = 0.002$ m, where k_s [m] is the sand-grain roughness height. Between cells, a growing aspect ratio of 20% is used. A minimum of 10 cells in the window edges are implemented. All the study cases (defined in section 6) can be reproduced with one grid. Figure 2a shows the base grid with 849,512 cells.

5.2. Boundary conditions

At the inlet, the profiles of $U(y)$, the turbulent kinetic energy $k(y)$, the turbulence dissipation rate $\varepsilon(y)$ and the specific dissipation rate $\omega(y)$ are calculated with as follows

$$U(y) = \frac{U_{abl}}{\kappa} \ln\left(\frac{y + y_0}{y_0}\right), \tag{7}$$

$$k(y) = a(I(y)U(y))^2, \tag{8}$$

$$\varepsilon(y) = \frac{U_{abl}^3}{\kappa(y + y_0)}, \tag{9}$$

$$\omega(y) = \frac{\varepsilon(y)}{C_\mu k(y)}, \tag{10}$$

where $U_{abl} = 0.52$ m/s is the atmospheric boundary layer friction velocity (value fitted from experiments), $y_0 = 2.82 \times 10^{-4}$ m the aerodynamic roughness length (value fitted from experiments), $\kappa = 0.42$ the von Karman constant, $a = 1.5$ the intensity turbulence factor (value selected from the sensitive analysis in section 5.4) and $C_\mu = 0.09$ an empirical constant [11].

At the ground and the building surfaces, the standard wall functions [14] with the roughness modification [15] are used. For the ground, k_s is calculated using the following expression [16]

$$k_s = \frac{9.793 y_0}{C_s} = 9.52 \times 10^{-4} \text{ m}, \tag{11}$$

where the roughness constant C_s is set with a value of 2.9. In the building, smooth surfaces are considered applying $k_s = 0$ and $C_s = 0.5$. Symmetry conditions are used at lateral and top domain surfaces and zero static pressure are set at outlet. Figure 2 shows views of the computational domain with the building.

5.3. Solver settings and parameters

The SIMPLEC algorithm is used for the pressure-velocity coupling. Second order discretization schemes are used for the convective and viscous terms of the governing and turbulence model equations. The convergence is considered achieved when all the scaled residuals are less than

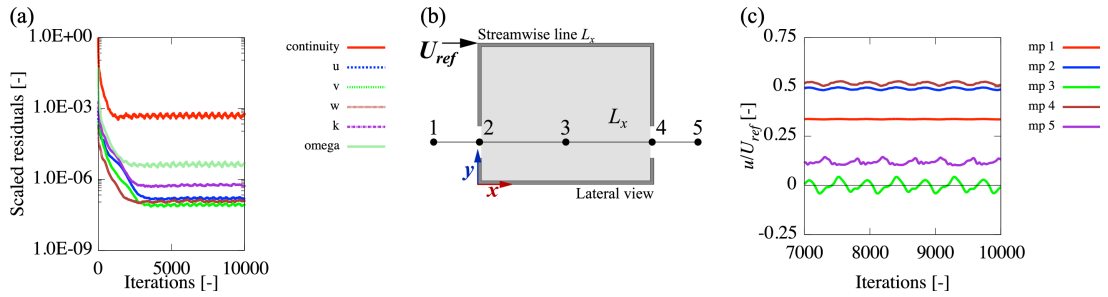

Figure 3. Variable monitoring along iterations for the reference case: (a) scaled residuals, (b) monitor point locations and (c) u/U_{ref} over the last 2,000 iterations.

10^{-3}. As stopping criterion, 10,000 iterations are set. Monitor points at outdoor, indoor and at the window locations are used to monitor u/U_{ref} and v/U_{ref} in all iterations. For the reference case, figure 3 shows the scaled residuals, the location of the monitor points and u/U_{ref} obtained from monitor points along the last 2,000 iteration. In these iterations, an oscillatory behavior around a constant value for all the scaled residuals, u/U_{ref} and v/U_{ref} is observed.

The streamwise gradients evaluation is done in the empty domain (without the building presence) to test the horizontal homogeneity of the incident profiles. In figure 1d, the incident numerical profiles of $U(y)$ and $I(y)$ are compared with their corresponding experimental profiles. The average difference between profiles is below 10%, fulfilling the recommended value [9].

5.4. Sensitive analyses

Three sensitive analyses are performed: for grid resolution, for turbulence model selection and for selection of turbulence intensity factor a. The course grid and the fine grid are built multiplying each spatial coordinate of the base grid by $\sqrt[3]{1/2}$ and $\sqrt[3]{2}$, respectively. The course grid has 418,912 cells and the fine grid 1,663,073 cells. A horizontal line across the building indoor at the midheight of the axial windows L_x is used for sensitivity analyses. The average difference of u/U_{ref} between course and base grids along L_x is 46%, while between base and fine grids is 6%. It is concluded that the base grid gives an accurate solution in a short computational time. For the turbulence model selection, the three most used turbulence models in NV studies are tested: Realizable $k-\varepsilon$, RNG $k-\varepsilon$ and SST $k-\omega$. The CFD and experimental results of u/U_{ref} along L_x are shown in figure 4a. The RNG $k-\varepsilon$ and SST $k-\omega$ show a good agreement with respect the experiment results, obtaining an average difference of u/U_{ref} of 6% and 5%, respectively. In this work, the SST $k-\omega$ turbulence model is selected. The last sensitive analysis is the test of three different values for $a = 0.5$, 1.0 and 1.5, in order to reproduce $k(y)$ (equation 8). A small sensitivity is obtained for a. The average difference of u/U_{ref} between the CFD and experimental results along L_x using $a = 0.5$ or 1.0 is 6%, while for $a = 1.5$ the difference is 5%. Figure 4b shows the qualitative comparison of the velocity vector fields at the vertical central plane between the experimental result and the CFD simulation. At indoor, the inflow jet with the downward direction, the small vortex formed in the left bottom corner and the large vortex above the inflow jet are numerically reproduced. In conclusion, the CFD simulation has an average difference of u/U_{ref} along L_x of 5%, using the base grid, the SST $k-\omega$ turbulence model and $a = 1.5$. Thus, the CFD simulation can be considered as validated.

6. Application example

The building geometry of the CFD validated simulation is taken as application example, considering it as an isolated educational building in a rural region of Mexico. The simulations of the application example are performed in laboratory scale. But conserving the geometric

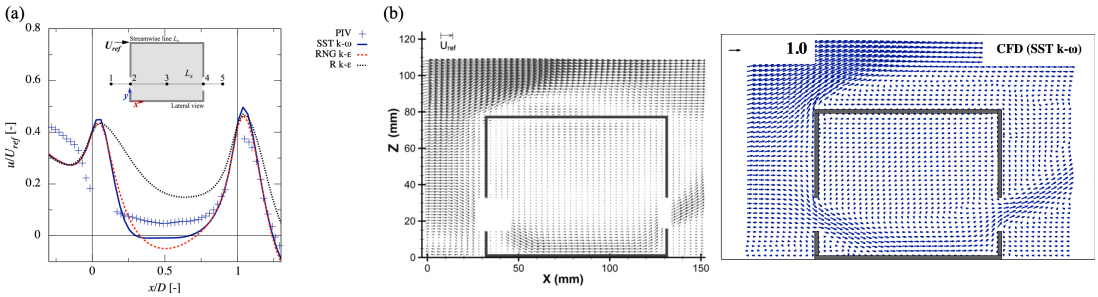

Figure 4. CFD simulation and experimental results: (a) comparison of u/U_{ref} along L_x for turbulence model selection and (b) velocity vector fields at the vertical central plane. For CFD, the base grid, the SST-$k-\omega$ turbulence model and $a = 1.5$ are used.

and dynamic similarities, the results can be expressed in full scale. A geometry scale factor of 37.5 is applied, giving a real scale building of 3.75 × 3.75 × 3.00 m^3 (width × length × height). The area of the windows is $A_w = 1.725 \times 0.675$ m^2 (width × height) and $P = 0.10$. The dynamic similarity is conserved by having the same Re_b as that in the experiments. Thus, $U_{ref} = 0.19$ m/s and $y_{ref} = 3.0$ m are employed. The value for U_{ref} considers a bad scenario for natural ventilation with low velocities of the wind. Four configurations of cross-ventilation are tested: axial, upward, corner and upward corner. All configurations have the windward window at bottom. The configurations axial and upward have one leeward window at bottom and top, respectively. While, configurations corner and upward corner have one lateral side window at bottom and top, respectively. The cross-ventilation configurations are shown in figure 5.

7. Evaluation of natural ventilation

The vertical central plane and the horizontal plane at 1.10 m height (corresponding to seated occupants head level) are selected for the NV evaluation. Figure 5 shows the velocity vector fields with contour plots of U/U_{ref} and the contour plots of $\overline{\tau_i}$ for all cross-ventilation configurations. It is observed that the inflow jet has a downward component close to the windward window. This jet is deflected by the interior side of the leeward facade and produces the upper vortex. For axial and upward configurations, the inflow jet is thinner and the upper vortex have small velocities. For axial configuration, the inflow jet easily reaches the leeward window and exits through it. For upward configuration, the deflected airflow goes up spread on the interior side of the leeward facade until it exits through the leeward window. For both configurations at the horizontal planes, in almost of the living zone U/U_{ref} is up to 0.2, with the exception of the windows and the interior side of the leeward facade. The lower $\overline{\tau_i}$ values are in the inflow jet as can be observed in the vertical planes. The small velocities in the upper vortex correspond to $\overline{\tau_i}$ above 8 min in almost all the living zone. For the corner and upward corner configurations, the inflow jet is wider having higher velocity, the upper vortex also has higher velocity compared with the axial and upward configurations. A decrement of the size of the air stagnation zone is clearly observed in the horizontal planes. Thus, lower values of $\overline{\tau_i}$ are obtained in the leaving zone with respect to the axial and upward configurations.

In table 1, the values of ACH, ARH and R for all configurations are summarized. Note that ACH consider an ideal piston flow, while ARH and R take into account the indoor airflow distribution. The four cross-ventilation configurations have small difference of ACH. According to this parameter, the configuration order from best to worst is: axial $ACH = 10.1$ 1/h, corner $ACH = 9.8$ 1/h, upward and upward corner $ACH = 9.4$ 1/h. The NV standard states for educational buildings in Mexico a minimum value of 6 ACH [3], thus all configuration overpass the standard requirement. When using the NV parameters that consider the indoor

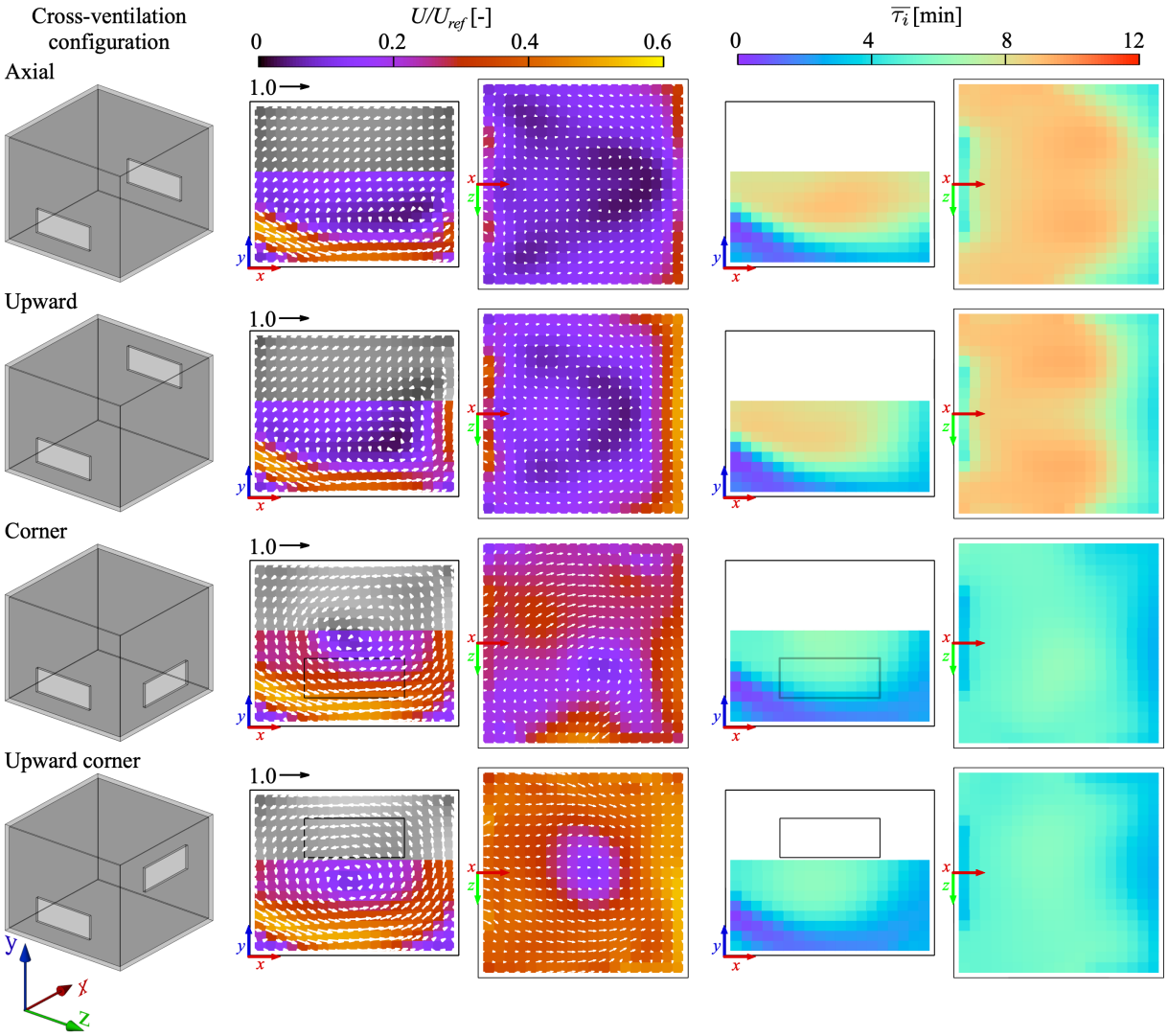

Figure 5. Four configurations of cross-ventilation of the application example. Results of velocity fields and local mean age of air $\overline{\tau_i}$ in the living zone (vertical central plane and horizontal plane at 1.10 m height).

airflow distribution, the differences between the four cross-ventilation configurations are larger. According to these parameters, the configuration order from best to worst is: corner ARH = 5.7 1/h and $R = 96\%$, upward corner $ARH = 5.7$ 1/h and $R = 94\%$, upward $ARH = 3.6$ 1/h and $R = 42\%$ and axial $ARH = 3.6$ 1/h and $R = 39\%$. ACH overestimates the air renovations per hour given by ARH, because ACH considers an ideal piston flow which is a nonrealistic approximation. The results of the present work show that NV evaluation using ACH can lead to wrong decisions. According to this parameter, the best configuration is the axial one, while it is the worst configuration according to ARH and R.

8. Conclusion

The natural ventilation (NV) evaluation of an educational building located in a rural region of Mexico is presented. The evaluation is preformed using validated CFD simulations. Four cross-ventilation configurations are compared: axial, upward, corner and upward corner. The

Table 1. Natural ventilation evaluation using the ideal piston flow consideration and AoA.

Configuration	ACH [1/h]	ARH [1/h]	R [%]
Axial	10.1	3.6	39
Upward	9.4	3.6	42
Corner	9.8	5.7	96
Upward corner	9.4	5.7	94

evaluation parameters are the air changes per hour ACH, the air renovation per hour ARH and the renovation parameter R. ACH considers an ideal piston flow and ARH and R are age or air associated parameters proposed in the present work.

In terms of ACH, the four cross-ventilation configurations have not significant differences in NV performance, being the axial configuration the better one. According to ARH and R, the configurations have larger performance differences. The configuration order from best to worst is corner, upward corner, upward and axial. The results of the present work show that NV evaluation using ACH can lead to wrong decisions. Thus, an improvement of the NV standard considering indoor airflow distribution parameters, as the ones proposed in this work, is recommended. The incorporation of these parameters can lead to the design of NV that promotes air movement in all the living zone, which improves the indoor air quality reducing pollutants and infectious particles like SARS-CoV-2 (responsable of COVID-19) and increases thermal comfort.

Acknowledgments
This work was partially supported by the CONACYT-SENER FSE-2017-01-291600 project. S F Díaz-Calderón acknowledges the scholarship PBEP grant by UNAM. J A Castillo acknowledges the postdoctoral fellowship grant by the CONACYT-SENER FSE-2017-01-291600 project.

References

[1] Sakiyama N, Carlo J, Frick J and Garrecht H 2020 *Renew. Sustain. Energy Rev.* **130** 109933
[2] Bhagat, Rajesh K and Davies Wykes, M S and Dalziel, Stuart B and Linden, P F 2020 *J. Fluid Mech.* **903** F1
[3] NTC-RC-CDMX 2011 *Norma Técnica Complementaria para el Proyecto Arquitectónico del Reglamento de Construcciones de la Ciudad de México* (Ciudad de México: Gobierno CDMX)
[4] Montazeri H and Montazeri F 2018 *Renew. Energy* **118** 502 – 20
[5] Kosutova K, van Hooff T, Vanderwel C, Blocken B and Hensen J 2019 *Build. Environ.* **154** 263–280
[6] Etheridge D and Sandberg M 1996 *Building ventilation: Theory and Measurements* (United Kingdom: John Wiley & Sons)
[7] Karava P, Stathopoulos T and Athienitis A 2011 *Build. Environ.* **46** 266 – 79
[8] Castillo J A 2021 Class notes: First steps in Fluent 19.0 `http://gee.ier.unam.mx/jacat/notes/` Last check. Feb. 2021
[9] Blocken B 2015 *Build. Environ.* **91** 219 – 45
[10] Ramponi R and Blocken B 2012 *Build. Environ.* **53** 34 – 48
[11] Tominaga Y, Mochida A, Yoshie R, Kataoka H, Nozu T, Yoshikawa M and Shirasawa T 2008 *J. Wind Eng. Ind. Aerodyn.* **96** 1749 – 61
[12] van Hooff T and Blocken B 2010 *Environ. Model. Softw.* **25** 51 – 65
[13] Castillo J A, Huelsz G, van Hooff T and Blocken B 2019 *Build. Simul.* **12** 475–88
[14] Launder B and Spalding D 1974 *Comput. Methods Appl. Mech. Eng.* **3** 269 – 89
[15] Cebeci T and Bradshaw P 1977 *Momentum transfer in boundary layers* (New York: Hemisphere Pub. Corp.)
[16] Blocken B, Stathopoulos T and Carmeliet J 2007 *Atmos. Environ.* **41** 238 – 52